JOURNAL OF THE ROYAL SOCIETY Interface

J. R. Soc. Interface (2010) **7**, 475–484
doi:10.1098/rsif.2009.0218
Published online 12 August 2009

Use of computational fluid dynamics to study forces exerted on prey by aquatic suction feeders

Tyler Skorczewski[1,*], Angela Cheer[1], Samson Cheung[1] and Peter C. Wainwright[2]

[1]*Graduate Group in Applied Mathematics, and* [2]*Department of Evolution and Ecology, University of California Davis, One Shields Avenue, Davis, CA 95616, USA*

Suction feeding is the most commonly used mechanism of prey capture among aquatic vertebrates. Most previous models of the fluid flow caused by suction feeders involve making several untested assumptions. In this paper, a Chimera overset grids approach is used to solve the governing equations of fluid dynamics in order to investigate the assumptions that prey do not interact with the flow and that the flow can be modelled as a one-dimensional flow. Results show that, for small prey, both neglecting the prey and considering prey interaction give similar calculated forces exerted on the prey. However, as the prey item increases in size toward the size of the gape, its effect on the flow becomes more pronounced. This in turn affects both the magnitude of the hydrodynamic forces imparted to the prey and the time when maximum force is delivered. Maximum force is delivered most quickly to intermediate sized prey, about one-third of mouth diameter, and most slowly to prey less than 7 per cent or greater than 67 per cent of mouth diameter. This suggests that the effect of prey size on the timing of suction forces may have substantial consequences for the feeding ecology of suction feeders that are known to prefer prey between 25 and 50 per cent of mouth diameter. Moreover, for a 15 cm fish with a 15 mm gape, assuming a radial one-dimensional flow field can result in underestimating the maximum force exerted on a 5 mm diameter spherical prey 1 gape distance from the mouth by up to 28.7 per cent.

Keywords: fish; suction feeding; computational fluid dynamics; aquatic prey capture

1. INTRODUCTION

Of the common methods of prey capture in fish, suction feeding is the most widespread (Liem 1990; Ferry-Graham *et al.* 2003). Suction feeding is an explosive event where a fish rapidly expands its buccal cavity in order to induce water flow into its mouth, and it is through the interaction with this flow field that the prey is drawn into the fish's mouth. Much work has been done on the musculoskeletal systems that fish use to generate this flow (Svänback *et al.* 2002; Bishop *et al.* 2008). Recently, increased attention has been given to describing the properties of the flow field itself (Ferry-Graham *et al.* 2003; Day *et al.* 2005, 2007; Higham *et al.* 2006; Wainwright *et al.* 2007; Van Wassenbergh & Aerts 2008, 2009) and the forces resulting from this flow (Wainwright & Day 2007; Holzman *et al.* 2008*a*,*b*). It is important to have an accurate understanding of the flow field as it is through this flow that fish impart force onto the prey.

Models of the flows generated by aquatic suction feeders are potentially valuable tools in the study of suction feeding performance (Muller *et al.* 1982). They can be used in a variety of simulation studies to examine the effects of prey morphology or prey and predator behaviour on the forces that are exerted on the prey by the suction feeder (Holzman *et al.* 2007, 2008*a*,*b*; Wainwright & Day 2007; Van Wassenbergh & Aerts 2008, 2009). Models of suction flow patterns permit the exploration of parameter space and can lead to insights into animal diversity and the underlying physics involved in the suction feeding mechanism.

In all previous models of the flow induced by suction feeding, assumptions were made so that quantitative insights became tractable. A common assumption is the rotational symmetry of the system (Weihs 1980; Muller *et al.* 1982; Drost *et al.* 1988*a*; Wainwright & Day 2007; Van Wassenbergh & Aerts 2009). Inviscid flow is assumed in some studies (Weihs 1980; Muller *et al.* 1982; Wainwright & Day 2007). Other assumptions deal with the shape of the mouth. For example, the mouth is modelled as one point in space (Weihs 1980; Wainwright & Day 2007), or by a circular ring vortex (Muller *et al.* 1982). When dealing with the prey item, assumptions include treating the prey as a particle of fluid (Weihs 1980; Muller *et al.* 1982;

*Author for correspondence (tskorc@math.ucdavis.edu).

Received 5 June 2009
Accepted 17 July 2009

Drost *et al.* 1988*b*) and assuming the prey does not interact with the flow (Wainwright & Day 2007). Both assumptions allow the prey to be neglected when calculating the flow field.

Advances in computation now allow for simulation of full three-dimensional viscous fluid flows where the prey interacts with the flow. Recently, computational fluid dynamics (CFD) techniques were used to illustrate consequences of a viscous flow, to show that the prey item can influence properties of the flow, and to reveal some consequences of laminar versus turbulent flow in suction feeding events (Van Wassenbergh & Aerts 2009). In the present paper, CFD is used to simulate the flow field resulting from the suction feeding event of a fish feeding on a stationary spherical prey, and to calculate the resulting forces acting upon the prey. The three-dimensional computations include the interaction of the prey with the flow generated by the fish. Unlike previous studies, the description of the flow field is fully three dimensional and is not limited to only the radial distance from the centre of the mouth. With a one-dimensional set-up the flow field implicitly assumes that the fish mouth behaves as a point sink, where all water enters the fish mouth through one point in space. In our three-dimensional calculations the mouth opening is modelled as a disc with non-zero area, more closely reflecting the geometry of a suction feeding fish. The results of these three-dimensional viscous computations, including prey interaction, are compared with the results of a previously published one-dimensional inviscid model that does not include prey interaction (Wainwright & Day 2007). Since it is through the prey's interaction with the fluid flow generated by suction that the prey feels force, it is important to investigate how neglecting this interaction when calculating the flow field affects prey capture by suction feeding fishes. Previous CFD models (Van Wassenbergh & Aerts 2009) are effectively two-dimensional because of the assumption of rotational symmetry of the flow. Also, different forces that result from the suction flow were not explicitly calculated and compared in previous studies. From fluid dynamics principles we argue that prey interaction is important to the modelling of suction feeding flows and our results show that as the size of the prey increases its effects on the flow become more pronounced.

2. METHODOLOGY

The approach taken to simulate a suction feeding event is as follows. First, for each time step of the simulation, the complete three-dimensional viscous fluid flow field is calculated. To simulate suction, a time-dependent velocity is imposed on the boundary of the computational mesh that represents the mouth of the fish. This prescribed suction velocity peaks 30 ms after the onset of the strike and has a duration of 60 ms. Two types of forces exerted on the prey are then calculated: a drag force and an acceleration reaction force. Second, time is advanced, a new suction velocity is imposed at the mouth opening, a new flow field is calculated and the resulting forces are computed. This is repeated until the end of the suction feeding event.

2.1. Governing equations

The equations that govern the flow of water during a suction feeding event are the incompressible Navier–Stokes equations. They express conservation laws for mass and momentum and are presented in primitive variable (velocity and pressure) formulation as

$$\nabla \cdot \vec{u} = 0, \tag{2.1}$$

$$\frac{\partial u_i}{\partial t} + (\vec{u} \cdot \nabla) u_i = \frac{-1}{\rho} \nabla p + \nu \nabla^2 u_i. \tag{2.2}$$

Here $\vec{u} = (u, v, w)^{\mathrm{T}}$ is the fluid velocity vector, u_i is an individual component of the velocity vector, p is the pressure, $\rho = 1000$ (kg m^3) is the density of water, and $\nu = 10^{-6}$ (m^2 s^{-1}) is the kinematic viscosity. These equations are a system of coupled nonlinear partial differential equations. There are currently very few analytical solutions to these equations and only for simple geometries. These equations are also notoriously hard to solve numerically (Kwak *et al.* 2005). The continuity equation, $\nabla \cdot \vec{u} = 0$, represents the incompressible nature of the fluid and is an elliptic equation. With elliptic equations, changes in boundary conditions are felt throughout the flow domain instantaneously. For the problem of simulating suction feeding, having the prey interact with the flow requires adding no slip boundary conditions at the location of the prey. This means that prey interaction affects the flow field everywhere. However, in Van Wassenbergh & Aerts (2009), significant alterations to the flow field are shown to be confined to regions close to the boundaries of the fish mouth and prey body in suction feeding flows. These changes to the flow field, close to the prey body, influence the hydrodynamic force calculations as the force calculations are primarily concerned with the flow near the prey.

The approach taken to obtain a numerical solution for the flow equations follows the method described in Pandya *et al.* (2003). The method is based on using a diagonalized, alternating direction implicit, beam warming, approximate factorization scheme to obtain a numerical solution of the Navier–Stokes equations (Tannehill *et al.* 1997). Low Mach number preconditioning is used to improve the solution accuracy since the fluid speeds resulting from suction feeding are more than three orders of magnitude smaller than the sound speed in water. This method allows for variable density; however, with the low Mach number preconditioning, the density is kept essentially constant, $\rho = 1000 \pm 0.04$ kg m^{-3}. This method is implemented in the OVERFLOW software package developed at NASA Ames (Buning 2002). Calculations were performed on a four processor Linux computer.

Once the flow field is obtained we calculate the forces on the prey. The force on the prey is decomposed into two parts: the drag force and the acceleration reaction force. The drag force at a fixed time t is based upon the flow field at time t, and the acceleration reaction

force arises because the flow field is changing in time. The drag force is calculated as in Acheson (1990)

$$F_{\mathrm{d}} = \int \boldsymbol{\sigma} \cdot \vec{n}\, \mathrm{d}A, \tag{2.3}$$

where $\vec{n}$ is the normal vector, and the stress tensor, $\boldsymbol{\sigma}$, is given by

$$\boldsymbol{\sigma}_{ij} = -P\delta_{ij} + \boldsymbol{\mu}\left(\frac{\partial u_i}{\partial x_j} + \frac{\partial u_j}{\partial x_i}\right). \tag{2.4}$$

The acceleration reaction force from Denny (1988) is given by

$$F_{\mathrm{ar}} = (1 + C_{\mathrm{a}})\boldsymbol{\rho} V_{\mathrm{p}} \frac{\mathrm{D}u}{\mathrm{D}t}. \tag{2.5}$$

Here C_{a} is the added mass coefficient (0.5 for a sphere), $\boldsymbol{\rho}$ is the density of water, V_{p} is the volume of the prey and $\mathrm{D}/\mathrm{D}t$ is the material derivative. The value for $\mathrm{D}u/\mathrm{D}t$ is obtained by taking the average around a volume encompassing the prey item.

We note that while we calculate two forces (drag, equation (2.3), and acceleration reaction, equation (2.5)), the model presented in Wainwright & Day (2007) has three forces—a drag force, an acceleration reaction force and a pressure gradient force. The two forces calculated here are related to the three forces in the Wainwright and Day model (now referred to as the WD model) in the following way. The drag force in the WD model is given by

$$F_{\mathrm{d,WD}} = \frac{1}{2}\boldsymbol{\rho} U^2 A_{\mathrm{f}} C_{\mathrm{d}}, \tag{2.6}$$

where U is the speed of the fluid relative to the speed of the prey, A_{f} is the frontal area of the prey and C_{d} is an experimentally determined drag coefficient. Equation (2.6) is analogous to the drag force given by equation (2.3) and is used to calculate the drag on a body in a quasi-steady, uniform flow. A uniform flow assumption may be acceptable for prey much smaller than the mouth aperture of the fish; however, a suction feeding event does not generally produce a uniform flow due in part to the size and shape of the fish body. The WD model assumes that a steady stress field develops and differs from the current model, which calculates drag based on an unsteady stress field. The WD drag model also assumes that the prey moves either directly with the flow or directly against it. Any movement not in these directions is ignored. Calculating drag by integrating stress over the surface area, equation (2.3), is not limited to these constraints.

The acceleration reaction force of the model presented here, equation (2.5), is the sum of the acceleration reaction force and the pressure gradient force of the WD model. The acceleration reaction force of the WD model for stationary prey is given by

$$F_{\mathrm{ar,WD}} = C_{\mathrm{a}} V_{\mathrm{p}} \boldsymbol{\rho} \frac{\mathrm{D}u}{\mathrm{D}t} \tag{2.7}$$

and the pressure gradient force is given by

$$F_{\mathrm{pg,WD}} = -L_x A_{\mathrm{f}} \frac{\mathrm{d}p}{\mathrm{d}x}, \tag{2.8}$$

where

$$\frac{\mathrm{d}p}{\mathrm{d}x} = -\boldsymbol{\rho}\left(\frac{\partial u}{\partial t} + u\frac{\partial u}{\partial x}\right) = -\boldsymbol{\rho}\frac{\mathrm{D}u}{\mathrm{D}t}. \tag{2.9}$$

Since $L_x A_{\mathrm{f}} = V_{\mathrm{p}}$, we see

$$F_{\mathrm{ar}} = F_{\mathrm{ar,WD}} + F_{\mathrm{pg,WD}}. \tag{2.10}$$

The pressure gradient force of the WD model implicitly makes the assumption of inviscid flow, since it ignores viscous terms in the momentum equation used to calculate the pressure gradient.

2.2. Chimera overset grids

The computational mesh, where the solution of the system of fluid flow equations is approximated, is a set of Chimera overset grids. In this set-up (figure 1) one large complex grid is replaced with a set of simpler, smaller, body fitted and overlapping grids. The smaller grids are of two types—near body grids and off body grids. Near body grids are generated so that solutions accurately represent fluid near solid bodies. Off body grids represent the surrounding fluid. In some cases grid points of one grid would lie inside the solid body defined by another grid. These are called hole points. Calculations are not performed on these points. Points where two grids overlap are called fringe points. When solving the equations, fringe points are solved inside their respective grids, and then tri-linear interpolation is used to interpolate their values to the overlapping grids. For static grids, the software package PEGASUS from NASA Ames is used to track interior and fringe points (Rogers *et al.* 2003).

2.3. Validation

In order to make sure our numerical software accurately simulates suction feeding flows, our calculations of suction feeding flows are validated against experimental data. Suction feeding data from a 15 cm bluegill (*Lepomis macrochirus*) from a previously published particle image velocimetry (PIV) experiment (Wainwright & Day 2007) are used for this comparison. This experiment shows that the fluid speed along the centreline emanating from the middle of the mouth can be expressed as

$$\mathrm{FS}(x,t) = \mathrm{FS}_{\mathrm{mouth}}(t)(0.098x^4 - 0.70x^3 + 1.86x^2 - 2.19x + 1), \tag{2.11}$$

where x is the distance from the mouth normalized by gape, and $\mathrm{FS}_{\mathrm{mouth}}(t)$ the fluid speed at the mouth at different times.

The Chimera grid set-up used for these calculations is similar to the one shown in figure 1 except without the prey grid. For this case the fish is stationary (i.e. it is not swimming toward the prey item during the strike), and a time dependent suction velocity is imposed on the boundary of the mouth of the fish. The profile of this boundary condition is shown in figure 2. The velocity on the centreline is extracted from the computed solution at several times and compared with the PIV

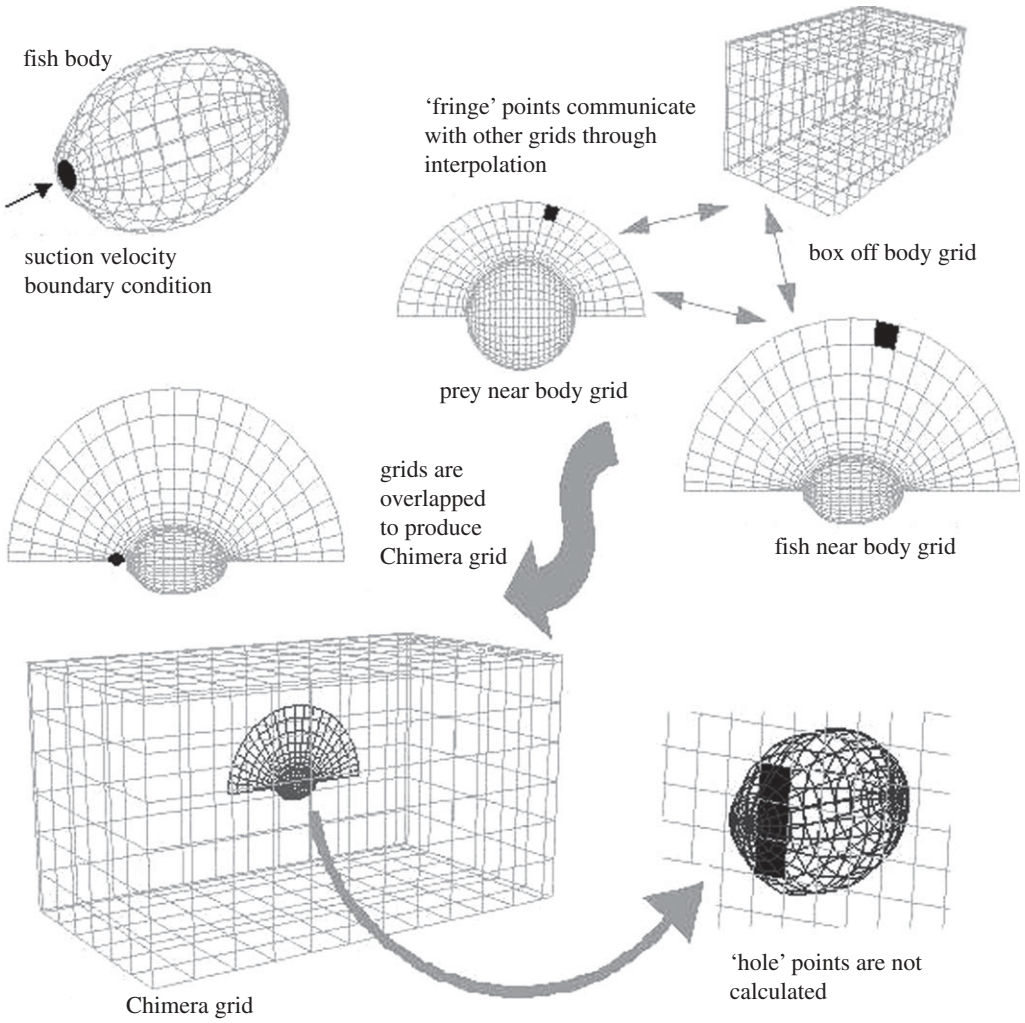

Figure 1. Chimera overset grids are used to represent the fish, prey and flow field. The fish is represented by an ellipsoidal shape and the grid surrounding the fish is created using a hyperbolic grid generation technique. A similar spherical grid is used to represent the prey and the flow field around the prey. These grids are embedded into a large box grid representing the surrounding fluid. The outer boundary of the overlapping grids are called fringe points and the points of the box grid that lie inside the fish or the prey are holes. Holes are ignored in the calculations.

results. Comparisons are performed at $t = 20$ ms, before the time of peak suction, at $t = 30$ ms, the time of peak suction, and at $t = 40$ ms, after the time of peak suction. The fluid velocity normalized to the fluid speed at the mouth versus the distance from the mouth normalized to gape show strong agreement with the experimental data (figure 3). The results also display the same property of a single spatial function (normalized to gape) scaled by the velocity at the mouth. This spatial function agrees well with the polynomial from the PIV results (equation (2.11)). The error, measured using the max norm, in the normalized fluid speed is 0.060068.

2.4. Simulations

A framework, similar to above, is used to perform simulations that explore two parameter spaces. The first set of computations is used to examine how the size of the prey affects the flow fields and the second set is used to examine the magnitude of the forces exerted on the prey, as a result of a suction feeding event, from a 15 cm long stationary bluegill with a 15 mm gape. The suction profile used for the boundary condition is shown in figure 2 and represents a 60 ms strike with peak suction occurring 30 ms after the onset of the strike. Spherical prey of several diameters, $d = 1$, 2.5, 5, 10 mm, are placed one gape distance (15 mm) away from the mouth along the centreline extending from the centre of the mouth. Distance is measured from the centre of the prey item to the centre of the fish mouth. After the flow field is obtained, forces on the prey for each case are calculated using equations (2.3) and (2.5) and are compared with those calculated by the WD model. The times of peak force exerted on the prey are measured from the onset of the strike.

The WD model assumes a radially symmetric flow field (Day *et al.* 2005). For our computations a snapshot of the flow field without prey is used to investigate the validity of this assumption. Velocity data along lines emanating from the centre of the mouth in the x–z plane at several angles ($\theta = 0^\circ$, 15°, 30°, 45°) are extracted, and the magnitude of the velocity component that lies on that line is calculated, i.e. $\vec{u} \cdot \hat{r}$, where $\hat{r}$ is the unit vector along the radial line (figure 4). In these

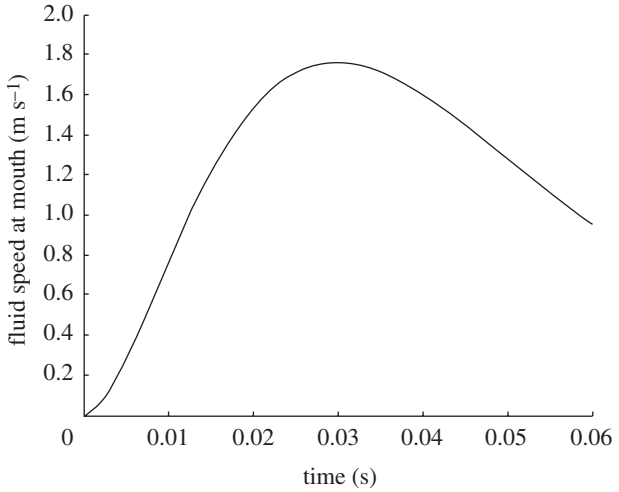

Figure 2. Time-dependent suction profiles. The time-dependent velocities during the suction event are prescribed as a boundary condition on the grid representing the opening of the fish mouth.

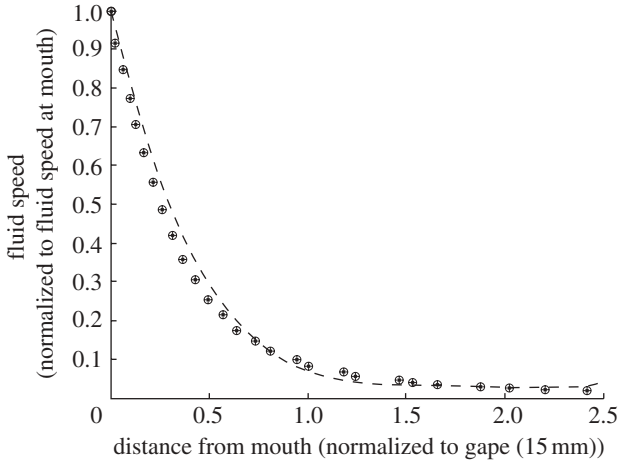

Figure 3. The simulation of a 15 mm bluegill sunfish suction feeding event is compared with particle image velocimetry (PIV) data of the same event. Fluid speed (normalized to the speed at the mouth) is plotted against the distance from the mouth (normalized to the gape along the centreline extending from the fish mouth). The PIV results (dashed line) show that, for all times, this relation can be represented by one curve. That is, flow can be described by a function of one space and one time variable. Simulation data for the centreline extending from the fish mouth is extracted at three different times: 0.02 s (o), 0.03 s (+) and 0.04 s (x) and plotted. For all three times, the calculations closely approximate the experimental data, validating the model.

calculations, radial symmetry is not present near the mouth because the mouth is not acting as a point sink for the flow. The inflow region has cross-sectional area related to the diameter of the mouth aperture. Whether this affects the forces exerted on the prey is investigated by placing a 5 mm diameter spherical prey at 1 gape distance, 15 mm, from the centre of the mouth at different angles in the x–z plane. The same suction boundary condition as above is used. The forces are calculated using equations (2.3) and (2.5) and compared with the forces calculated using the WD model.

3. RESULTS

3.1. Prey size

The results of the computation show that as the prey size increases the flow field with prey interaction deviates significantly from the flow field without prey (figure 5). For these simulations, the same suction profile as used for the validation calculations is used (figure 2), with the maximum suction velocity occurring 30 ms after the onset of the suction feeding event. Forces on the prey for each case are calculated and are compared with those calculated by the WD model (table 1, figure 6). These results show that as the prey diameter is halved the magnitude of the force exerted on the prey decreases by an order of magnitude. This is expected as the force scales as $O(r^3)$ and $(1/2)^3 \approx 1/10$. The most significant differences between the three-dimensional viscous model with the prey interacting with the flow field and the WD model with no interaction occur for prey sizes with diameters of 5 and 10 mm. The 1 and 2.5 mm diameter prey are much smaller than the 15 mm gape, and are probably small enough to be treated as fluid elements instead of interacting bodies. However, as the prey size increases, the regions of low flow behind the spherical prey are large enough to cause a significant deviation from the flow field without prey.

3.2. $\mathrm{D}u/\mathrm{D}t$ *calculations*

Two methods are used to calculate the value of $\mathrm{D}u/\mathrm{D}t$ in equation (2.5). One involves averaging over a volume encompassing the prey. This is implemented by using the values of $\mathrm{D}u/\mathrm{D}t$ on the near body grid representing the fluid around the prey. This method accounts for the prey's effect on the flow field. The average value for $\mathrm{D}u/\mathrm{D}t$ calculated depends on the size of the volume used in the average. As this volume increases, the time when the peak acceleration reaction force occurs converges to values between 9 and 10 ms for all prey sizes. However, the magnitude of the acceleration reaction force increases as the volume is increased. As a result, the acceleration reaction forces dominate with regard to the timing of when the peak total force occurs, since total force is the sum of acceleration forces and drag forces. Drag forces on the other hand always peak at the same time as peak suction, which is at $t = 30$ ms for this investigation. As the volume is increased the timing of peak total forces converges to the values shown in table 1.

The other method investigated involves calculating the value of $\mathrm{D}u/\mathrm{D}t$ by averaging over a circular ring of points perpendicular to the line connecting the centre of mass of the prey and the centre of the fish mouth. As this ring increases in size, the time when the peak acceleration reaction force occurs also converges to a value between 9 and 10 ms for all prey sizes, but the magnitude of these forces decreases. This is expected as the grid points used in the calculation are in locations of very slow fluid speed. As a result, the time when peak total force occurs coincides with the time of peak drag force. Peak drag force occurs at

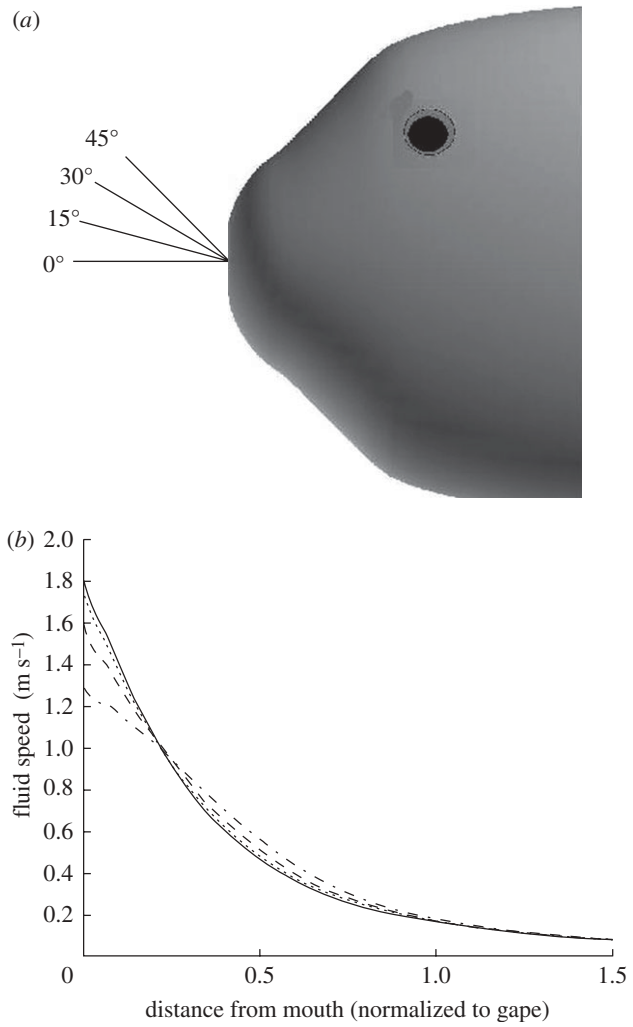

Figure 4. The impact of a point sink mouth assumption. A suction feeding event without prey interaction is simulated using the suction boundary condition of figure 2. Four lines emanating from the centre of the mouth at different angles are examined (*a*). The fluid speed along the ray is plotted against the distance from the mouth (normalized to gape) (*b*). Far from the mouth (>1 gape distance), all of the plots converge to the same value. Close to the mouth (<0.5 gape distance) the fluid speed along these rays decreases as the angles increase. Since the prey is located close to the mouth during a suction feeding event, these changes result in significant changes in the forces exerted on the prey (solid line, 0°; dotted line, 15°; dashed dotted line, 30°; dashed line, 45°).

the time of peak suction velocity. This implies peak total force occurs at the time of peak suction velocity, which was not seen in the experiments (Holzman *et al.* 2007).

3.3. Three-dimensional effects

The maximum force exerted on the prey for the three-dimensional viscous model agrees well with the WD model for the zero angle case, as the two forces are only about 0.2 per cent apart (table 2). As the angle increases, the maximum force increases from 0.6991 mN at 0° to 0.8999 mN at 45°. This represents a 28.7 per cent difference in the maximum force exerted on the prey, which is unaccounted for in the WD model. This is because as the angle increases the prey moves closer to the edge of the mouth and experiences stronger suction forces, even though it is still the same distance from the centre of the mouth. This illustrates one of the limitations of modelling the mouth as a point source.

4. DISCUSSION

Recent attempts to model and analyse the hydrodynamic forces imparted by the fluid flow on the prey involve the use of a one-dimensional model that makes simplifying assumptions about the extension into a three-dimensional model (Wainwright & Day 2007). This model is further used to understand the mechanistic basis of forces exerted on prey by suction feeders and how alterations of the flow field affects these forces (Holzman *et al.* 2008*a*,*b*). For the prey sizes explored in this study, the three-dimensional CFD calculations indicate that the one-dimensional model provides an adequate approximation of the magnitude of forces experienced by the prey item provided that the prey is directly in front of the mouth. For this case the two models show strong agreement (i.e. they are within 10% of one another for the magnitude of forces) across the range of prey sizes studied (table 1). This suggests that the one-dimensional model can be used to estimate the magnitude of forces acting on the prey in a known flow field and with the prey directly in front of the mouth.

A larger discrepancy between the one-dimensional and three-dimensional models is found in the timing of the forces. At prey sizes with diameter 66 per cent of the diameter of the mouth aperture, or at very small sizes (7% of gape size), the time until peak force is almost doubled when compared with the one-dimensional WD model. When the prey dimensions are intermediate, as they typically are in empirical studies (Holzman *et al.* 2007, 2008*a*,*b*), the one-dimensional model is adequate in predicting the time when maximum forces are exerted on the prey. The marked increase in time to maximum forces at prey size above 66 per cent of gape diameter reflects the influence of the prey on the flow field. The flow field deviated significantly from the flow field with no fluid–prey interaction (figure 5).

We suggest that the effect of prey size on the timing of peak forces may have considerable ecological significance for feeding fishes. The implication of this result is that suction feeding performance is highest on intermediate-sized prey, at least with respect to how quickly the strike develops and the force that is exerted on the prey by the suction flow. Bluegill, like many suction feeding fishes, feed on a wide range of animal prey, including prey more than 66 per cent of the mouth diameter. Of the various prey sizes in this study, peak force is reached most quickly for the 5 mm diameter prey (33% of mouth diameter). At this prey size, peak force is reached 60 per cent sooner when compared with the cases of the largest and smallest prey. Size of the prey is shown to be a major factor in studies of

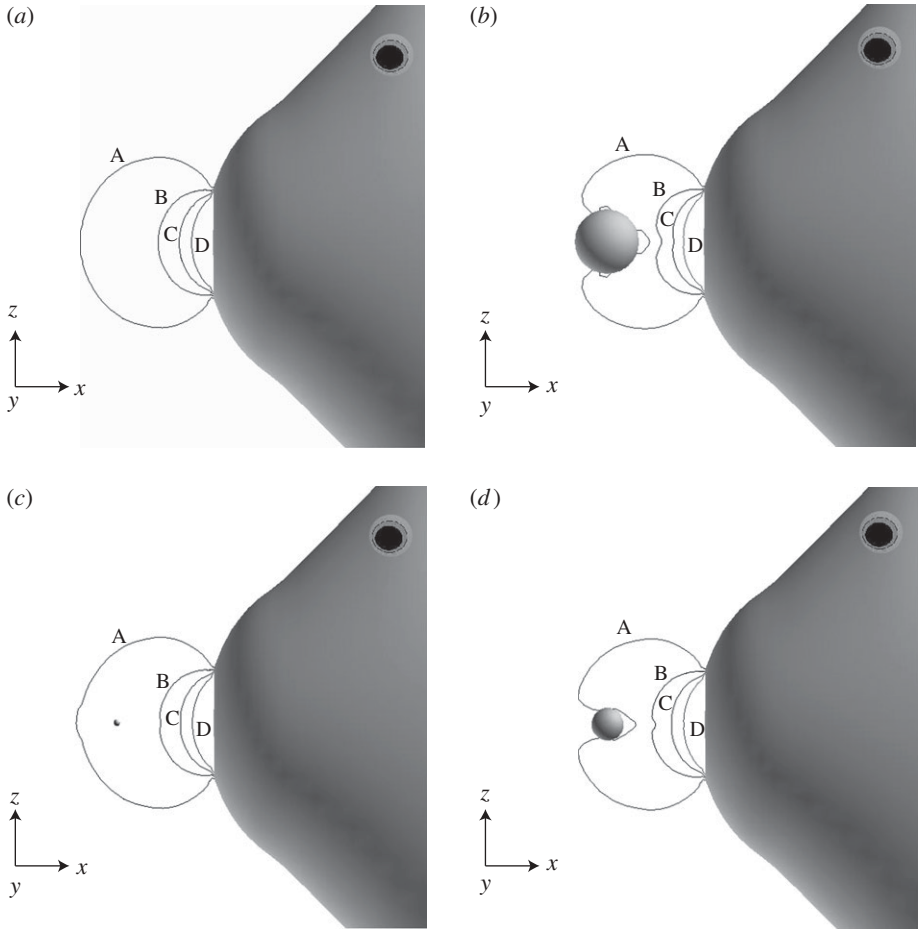

Figure 5. Contours of the x-component of velocity in front of the mouth of a suction feeding event without prey (a), with a 10 mm diameter prey (b), with a 1 mm diameter prey (c) and with a 5 mm diameter prey (d). The prey is located 1 gape distance from the centre of the mouth. Significant deviations in the contour lines are observed for the larger prey sizes. Allowing the prey to interact with the flow creates a region of recirculation behind the prey, which affects the forces exerted on the prey (A = 0.090, B = 0.393, C = 0.697, D = 1.000).

Table 1. Values of the maximum force and the time of maximum force calculated using the three-dimensional computational fluid dynamics model and the WD model. The results shown are for spherical prey of several diameters centred 1 gape distance away from the mouth. Times are measured from the onset of the strike. Both models give similar maximum forces. However, results of our three-dimensional calculation give longer times to maximum force.

diameter of spherical prey (mm)	maximum force in three-dimensional computation (mN)	time of maximum force in three-dimensional computation (ms)	maximum force in WD computation (mN)	time of maximum force in WD computation (ms)
10	5.381	19.0	5.478	10.0
5	0.7154	11.5	0.7008	10.0
2.5	0.09762	14.0	0.09073	10.5
1	0.009887	21.5	0.00618	12.5

fish prey selection (Werner & Hall 1974), and studies repeatedly show that fish prefer prey between 25–50 per cent of mouth diameter (Wainwright & Richard 1995; Turesson *et al.* 2002; Graeb *et al.* 2005). Prey in this size range offer the highest energy return for the energy spent pursuing, capturing and handling them (Werner 1974, 1977; Kislalioglu & Gibson 1976). The quicker time to peak forces exerted on prey for intermediate-sized prey provides another, previously unrecognized reason for the tendency for suction feeding fishes to feed on prey at this size range (between 25% and 50% of their mouth diameter; Keast & Webb 1966; Wainwright & Richard 1995). We emphasize that this insight is derived from use of the three-dimensional model that allows the body of the prey to influence the water flow. Our simulations without fluid–prey interactions did not show any difference in time to peak force.

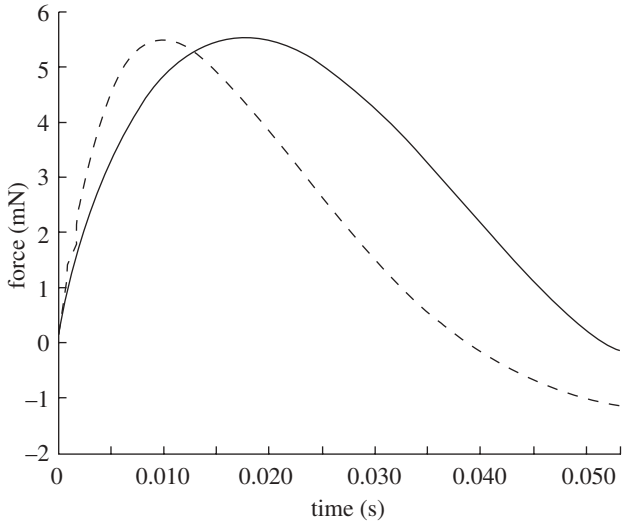

Figure 6. Plot of force versus time for a simulation of a suction feeding strike on a 10 mm spherical prey using two different models. The WD model (dashed line) gives a maximum force of 5.478 mN at 10 ms into the strike. The three-dimensional model (solid line) gives a similar maximum force of 5.381 mN at 19.0 ms into the strike, 90% longer than that for the WD model.

The limitations of assuming a point sink mouth geometry are shown by altering the position of the prey. As a 5 mm diameter prey is moved from 0° to 45° with respect to the line emanating from the centre of the mouth but kept at a distance equal to one gape diameter, the forces exerted on the prey change from 0.7154 to 0.8999 mN. This is an increase of up to 28.7 per cent when compared with the forces in the single point sink mouth, which cannot account for changes in position. While a point sink mouth may work well when describing the fluid flow far from the fish mouth in a suction feeding flow (Muller *et al.* 1982), the important attributes of the fluid flow occur within a very small volume that is very close to the fish mouth.

The increase in the magnitude of the force imparted to prey located at increasing angles may come at a cost. A recent CFD study (Van Wassenbergh & Aerts 2009) shows that, for certain mouth geometries, a region of separated flow may occur inside the expanding buccal cavity of a suction feeding fish and this could lead to better suction feeding performance for prey which moves through the centre of the buccal cavity during a strike. The trade-off between prey position and prey handling inside the buccal cavity is an area that should be addressed in future work. In addition, the results presented here do not take into account the head rotation that can occur in some fish suction feeding events, namely pipefish and seahorse strikes. Head rotation in this case would work to enhance the performance of the suction feeding event. It has been shown that, in pipefish, quick head rotation can lead to a decreased dependence on suction during a prey capture event (Van Wassenbergh & Aerts 2008).

Our study reveals effects of prey size and position on the forces that a suction feeder exerts on the prey, but we do not mean to imply that these are the only sources of variation in these forces that a predator can exploit. Suction feeding fishes approach their prey prior to the strike, by swimming forward and many fish also protrude their jaws toward the prey as they open their mouth and expand the buccal cavity. The simple model referred to here (the WD model) was used to dissect the relative impact of variation in swimming, jaw protrusion and the timing of the strike on variation in the forces exerted by suction feeders (Holzman *et al.* 2007). Swimming and jaw protrusion can enhance forces because they cause the velocity around the prey item to increase more rapidly than it would if the relative position of predator and prey are fixed at the onset of the strike. This increases the acceleration of fluid and hence the forces due to acceleration. Timing is also important because of the ephemeral nature of the suction flow. Peak suction velocity is maintained for only 2–3 ms during the strike and the maximum fluid acceleration occurs at a single moment during buccal expansion. The implication is that there is an optimal timing of the approach towards the prey that will maximize the forces that any given strike can exert on the prey. Because forces drop off rapidly around this maximum, the timing of the strike emerges as a key component of suction feeding performance in predator–prey encounters (Holzman *et al.* 2008*a*). Previous work shows that species differ both in force capacity and in the extent to which they time the approach to maximize the forces that they can exert with a given strike (Holzman *et al.* 2008*a*,*b*). One implication of the present study is that the insights gained from using the WD model in this context should not immediately be generalized to other prey sizes. An important goal in future research will be to determine whether the optimal strike strategy of suction feeders is prey-size dependent.

The insights gained from the CFD model indicate two general areas in which the strategies of potential prey animals may be most effectively focused to elude suction feeding predators. These are strategies that increase the sensitivity of prey to the hydrodynamic signals provided by attacking suction feeders, and strategies that minimize the forces experienced by the prey that is exposed to the suction flow. Many prey of suction feeding fishes are either crustaceans or other fishes and both of these groups have well-studied sensory structures or cells that are sensitive to sheer stress in the water, including sheer caused by the bow wake of an approaching predator or the suction flow itself. It is known that these stresses will cause the initiation of escape responses in copepods, for example, a common prey of plankton-feeding fishes (Kiorboe *et al.* 1999). One would expect that lineages of small crustaceans that are exposed to suction feeders would experience strong natural selection on the sensitivity of these sensory systems, allowing them to detect oncoming predators as soon as possible. A second strategy is to minimize forces experienced in the suction flow. Elongate body forms may help distribute body mass inside and out of the suction flow, reducing forces. Alternatively, body form may change in the face of the flow, temporarily reducing the forces experienced

Table 2. Values of maximum force and the time of maximum force calculated on a 5 mm spherical prey located 1 gape distance from the centre of the fish mouth at several angles using two different models. The WD model gives the same value for all cases. The three-dimensional model shows considerable differences in the maximum force calculated, up to 28.7% when compared with the WD model. This is attributed to the relaxing of the assumption of a point sink fish mouth assumed in the WD model.

angle (°)	maximum force in three-dimensional computation (mN)	time of maximum force in three-dimensional computation (ms)	maximum force in WD computation (mN)	time of maximum force in WD computation (ms)
0	0.7154	11.5	0.7008	10
15	0.7387	12.0	0.7008	10
30	0.8075	11.5	0.7008	10
45	0.8999	11.5	0.7008	10

in the flow. Such an effect is seen in some seaweeds that are exposed to waves and change their posture in a flow in such a way that reduces the forces they experience (Denny & Hale 2003). Future studies will be needed to determine the extent to which these alternative strategies have been pursued by various lineages of organisms that are preyed upon by suction feeding predators.

We would like to thank the referees for their helpful comments. This material is based upon work supported by the National Science Foundation under Grants DMS-0135345 and IOB-0444554.

REFERENCES

Acheson, D. 1990 *Elementary fluid dynamics*. Oxford, UK: Clarendon Press.

Bishop, K. L., Wainwright, P. C. & Holzman, R. 2008 Anterior to posterior wave of buccal expansion in suction feeding fish is critical for optimizing fluid flow velocity profile. *J. R. Soc. Interface* **5**, 1309–1316. (doi:10.1098/rsif.2008.0017)

Buning, P. 2002 *Overflow user's manual*. Hampton, VA: NASA Langley Research Center.

Day, S. W., Higham, T., Cheer, A. & Wainwright, P. C. 2005 Spatial and temporal patterns of water flow generated by suction-feeding bluegill sunfish *Lepomis macrochirus* resolved by particle image velocimetry. *J. Exp. Biol.* **208**, 2661–2671. (doi:10.1242/jeb.01708)

Day, S. W., Higham, T. & Wainwright, P. C. 2007 Time resolved measurements of the flow generated by suction feeding fish. *Exp. Fluids* **43**, 713–724. (doi:10.1007/s00348-007-0405-0)

Denny, M. 1988 *Biology and mechanics of the wave-swept environment*. Princeton, NJ: Princeton University Press.

Denny, M. W. & Hale, B. B. 2003 Cyberkelp: an integrative approach to the modelling of flexible organisms. *Phil. Trans. R. Soc. Lond. B* **358**, 1535–1542. (doi:10.1098/rstb.2003.1341)

Drost, M., Muller, M. & Osse, J. 1988*a* A quantitative hydrodynamical model of suction feeding in larval fishes: the role of frictional forces. *Proc. R. Soc. Lond. B* **234**, 263–281. (doi:10.1098/rspb.1988.0048)

Drost, M. R., Osse, J. W. M. & Muller, M. 1988*b* Prey capture by fish larvae, water flow patterns and the effect of escape movements of prey. *Neth. J. Zool.* **38**, 23–45. (doi:10.1163/156854288X00021)

Ferry-Graham, L., Wainwright, P. C. & Lauder, G. 2003 Quantification of flow during suction-feeding in bluegill sunfish. *Zoology* **106**, 159–168. (doi:10.1078/0944-2006-00110)

Graeb, D. S., Galarowicz, T., Wahl, D. H., Dettmers, J. M. & Simpson, M. J. 2005 Foraging behavior, morphology, and life history variation determine the ontogeny of piscivory in two closely related predators. *Can. J. Fish. Aquat. Sci.* **62**, 2010–2020. (doi:10.1139/f05-112)

Higham, T., Day, S. W. & Wainwright, P. C. 2006 Multidimensional analysis of suction feeding performance in fishes: fluid speed, acceleration, strike accuracy and the ingested volume of water. *J. Exp. Biol.* **209**, 2713–2725. (doi:10.1242/jeb.02315)

Holzman, R., Day, S. W. & Wainwright, P. C. 2007 Timing is everything: effects of kinematic variation on the force exerted by suction feeding bluegill on their prey. *J. Exp. Biol.* **210**, 3328–3336. (doi:10.1242/jeb.008292)

Holzman, R., Day, S. W., Mehta, R. S. & Wainwright, P. C. 2008*a* Jaw protrusion enhances forces exerted on prey by suction feeding fishes. *J. R. Soc. Interface* **5**, 1445–1457. (doi:10.1098/rsif.2008.0159)

Holzman, R., Collar, D. C., Day, S. W., Bishop, K. L. & Wainwright, P. C. 2008*b* Scaling of suction-induced flows in bluegill: morphological and kinematic predictors for the ontogeny of feeding performance. *J. Exp. Biol.* **211**, 2658–2668. (doi:10.1242/jeb.018853)

Keast, A. & Webb, D. 1966 Mouth and body form relative to feeding ecology in the fish fauna of a small lake, Lake Opinicon, Ontario *J. Fish. Res. Board Canada* **23**, 1845–1874.

Kiorboe, T., Saiz, E. & Visser, A. 1999 Hydrodynamic signal perception in the copepod Acartia tonsa. *Mar. Ecol. Progr. Ser.* **179**, 97–111. (doi:10.3354/meps179097)

Kislalioglu, M. & Gibson, R. N. 1976 Prey 'handling time' and its importance in food selection by the 15 spined stickleback, *Spinachia spinachia* (L.). *J. Exp. Mar. Biol. Ecol.* **25**, 115–158.

Kwak, D., Kiris, C. & Chang, S. 2005 Computational challenges of viscous incompressible flows. *Comput. Fluids* **34**, 283–299. (doi:10.1016/j.compfluid.2004.05.008)

Liem, K. 1990 Aquatic versus terrestrial feeding modes: possible impacts on the trophic ecology of vertebrates. *Am. Zool.* **30**, 209–221.

Muller, M., Osse, J. & Verhagen, J. 1982 A quantitative hydrodynamical model of suction feeding. *J. Theoret. Biol.* **95**, 49–79. (doi:10.1016/0022-5193(82)90287-9)

Pandya, S., Venkateswaran, S. & Pulliam, T. 2003 Implementation of preconditioned dual-time procedures in overflow. In: *41st Aerospace Sciences Meeting, Reno, NV, 5–9 January 2003*. Reston, VA: American Institute of Aeronautics and Astronautics.

Rogers, S., Suhs, N., Dietz, W., Nash, S. & Onufer, J. 2003 *Pegasus user guide*. Moffet Field, CA: NASA Ames Research Center, Microcraft, MCAT, Inc.

Svänback, R., Wainwright, P. & Ferry-Graham, L. 2002 Linking cranial kinematics, buccal pressure, and suction

feeding performance in largemouth bass. *Physiol. Biochem. Zool.* **75**, 532–543.

Tannehill, J., Anderson, D. & Pletcher, R. 1997 *Computational fluid mechanics and heat transfer*. Washington, DC: Taylor and Francis.

Turesson, H., Persson, A. & Bronmark, C. 2002 Prey size selection in piscivorous pikeperch (*Stizostdion lucioperca*) includes active prey choice. *Ecol. Freshwater Fish.* **11**, 223–233. (doi:10.1034/j.1600-0633.2002.00019.x)

Van Wassenbergh, S. & Aerts, P. 2008 Rapid pivot feeding in pipefish: flow effects on prey and evaluation of simple dynamic modelling via computational fluid dynamics. *J. R. Soc. Interface* **5**, 1291–1301. (doi:10.1098/rsif.2008.0101)

Van Wassenbergh, S. & Aerts, P. 2009 Aquatic suction feeding dynamics: insights from computational modelling. *J. R. Soc. Interface* **6**, 149–158. (doi:10.1098/rsif.2008.0311)

Wainwright, P. & Day, S. 2007 The forces exerted by aquatic suction feeders on their prey. *J. R. Soc. Interface* **4**, 553–560. (doi:10.1098/rsif.2006.0197)

Wainwright, P. C. & Richard, B. A. 1995 Predicting patterns of prey use from morphology with fishes. *Environ. Biol. Fishes* **44**, 97–113. (doi:10.1007/BF00005909)

Wainwright, P. C., Carroll, A. M., Collar, D. C., Day, S. W., Higham, T. E. & Holzman, R. 2007 Suction feeding mechanics, performance, and diversity in fishes. *Int. Comp. Biol.* **47**, 96–106. (doi:10.1093/icb/icm032)

Weihs, D. 1980 Hydrodynamics of suction feeding of fish in motion. *J. Fish Biol.* **16**, 425–433. (doi:10.1111/j.1095-8649.1980.tb03720.x)

Werner, E. E. 1974 The fish size, prey size, handling time relation and some implications. *J. Fish. Res. Board Canada* **31**, 1531–1536.

Werner, E. E. 1977 Species packing and niche complementarity in three sunfishes. *Am. Nat.* **111**, 553–578. (doi:10.1086/283184)

Werner, E. E. & Hall, D. J. 1974 Optimal foraging and the size selection of prey by the bluegill sunfish (*Lepomis macrochirus*). *Ecology* **55**, 1042–1052. (doi:10.2307/1940354)